

Are methane emissions from mangrove stems a cryptic carbon loss pathway? Insights from a catastrophic forest mortality

Luke C. Jeffrey¹ , Gloria Reithmaier¹ , James Z. Sippo¹ , Scott G. Johnston¹ , Douglas R. Tait¹ , Yota Harada²  and Damien T. Maher^{1,3} 

¹SCU Geoscience, Southern Cross University, PO Box 157, Lismore, NSW 2480, Australia; ²Australian Rivers Institute and School of Environment and Science, Griffith University, Gold Coast, 4215, Qld, Australia; ³School of Environment, Science and Engineering, Southern Cross University, PO Box 157, Lismore, NSW 2480, Australia

Summary

- Growing evidence indicates that tree-stem methane (CH₄) emissions may be an important and unaccounted-for component of local, regional and global carbon (C) budgets. Studies to date have focused on upland and freshwater swamp-forests; however, no data on tree-stem fluxes from estuarine species currently exist.
- Here we provide the first-ever mangrove tree-stem CH₄ flux measurements from >50 trees ($n = 230$ measurements), in both standing dead and living forest, from a region suffering a recent large-scale climate-driven dieback event (Gulf of Carpentaria, Australia).
- Average CH₄ emissions from standing dead mangrove tree-stems was $249.2 \pm 41.0 \mu\text{mol m}^{-2} \text{d}^{-1}$ and was eight-fold higher than from living mangrove tree-stems ($37.5 \pm 5.8 \mu\text{mol m}^{-2} \text{d}^{-1}$). The average CH₄ flux from tree-stem bases (c. 10 cm above-ground) was 1071.1 ± 210.4 and $96.8 \pm 27.7 \mu\text{mol m}^{-2} \text{d}^{-1}$ from dead and living stands respectively. Sediment CH₄ fluxes and redox potentials did not differ significantly between living and dead stands. Our results suggest both dead and living tree-stems act as CH₄ conduits to the atmosphere, bypassing potential sedimentary oxidation processes.
- Although large uncertainties exist when upscaling data from small-scale temporal measurements, we estimated that dead mangrove tree-stem emissions may account for c. 26% of the net ecosystem CH₄ flux.

Author for correspondence:

Luke C. Jeffrey

Tel: +61 (2) 6620 3000

Email: luke.jeffrey@scu.edu.au

Received: 9 April 2019

Accepted: 10 June 2019

New Phytologist (2019) **224**: 146–154

doi: 10.1111/nph.15995

Key words: carbon cycle, mangrove forest mortality, methane (CH₄), plant-mediated emissions, saline wetland, sediment diffusion, tree-stem fluxes.

Introduction

Methane (CH₄) is a potent greenhouse gas with a global warming potential 34–86 times that of carbon dioxide (CO₂) (Stocker *et al.*, 2013). Wetlands (which include mangrove and salt marsh ecosystems) are the largest natural source of atmospheric CH₄ (Saunois *et al.*, 2016). Most wetland CH₄ budgets and models have focused on diffusive fluxes (i.e. sediment and aquatic), ebullition and herbaceous plant-mediated emissions (Chanton *et al.*, 1989; Bartlett & Harriss, 1993; Bastviken *et al.*, 2008; Kirschke *et al.*, 2013; McNicol *et al.*, 2017). Only recently have tree stem CH₄ emissions been investigated as an important source of CH₄ to the atmosphere (Terazawa *et al.*, 2007; Covey *et al.*, 2012; Pangala *et al.*, 2015). Tree stem CH₄ emissions have been found to account for up to 50% of the Amazon basin CH₄ budget (Pangala *et al.*, 2017), and characterizing and quantifying tree stem CH₄ fluxes is now recognized as ‘a new frontier in the global carbon cycle’ (Barba *et al.*, 2019a).

Recent reviews of tree-mediated CH₄ emissions rely upon data synthesized from mostly living trees of freshwater wetlands, floodplains and upland forested origins (Barba *et al.*, 2019a; Covey & Megonigal, 2019). To date, very few studies have assessed CH₄ fluxes from standing dead tree stems (Carmichael

et al., 2014; Warner *et al.*, 2017) and/or saline wetlands. Furthermore, there is no consensus for the biophysical mechanisms transporting CH₄ along the soil–tree–atmosphere continuum (Barba *et al.*, 2019a), with debate continuing as to whether trees: act as passive pipes (diffusion) connecting the rhizosphere to the atmosphere; participate as active pipes (via xylem flow); or produce CH₄ internally in the heartwood (Covey *et al.*, 2012; Barba *et al.*, 2019b). Tree species, tree size, ecological adaptations, seasonality and hydrogeophysical context all likely play a role in the production and pathways of tree stem CH₄ flux (Keppler *et al.*, 2006; McLeod *et al.*, 2008; Pangala *et al.*, 2017; Pitz *et al.*, 2018). As an estimated 3.04 trillion trees exist globally (Crowther *et al.*, 2015), with c. 43% living in (sub) tropical forests (a region accounting for two-thirds of all natural CH₄ emissions), there is a growing consensus that tree-mediated CH₄ fluxes need to be quantified and considered in process-based models and global CH₄ budgets (Carmichael *et al.*, 2014; Saunois *et al.*, 2016).

Compared to freshwater wetlands, the CH₄ emissions from saline wetlands and mangrove forests have generally been considered negligible, as abundant sulfate (derived from seawater) favours sulfate reduction over methanogenesis (Burdige, 2012). Due to the high sedimentary carbon accumulation rates of

mangrove systems and ‘perceived’ low CH₄ emissions from saline wetlands, mangroves have historically been considered intensive ‘blue carbon’ sinks (Donato *et al.*, 2011; Sanders *et al.*, 2016; Lovelock & Duarte, 2019). Rosentreter *et al.* (2018), however, recently showed that global mangrove CH₄ emissions may partially offset ‘blue carbon’ burial by up to 20%, even though no tree-mediated fluxes were included in their synthesis. As the terrestrial–oceanic boundary represents an extremely dynamic and challenging environment, mangrove forests are subjected to frequent meteorological and physicochemical stressors, which can be exacerbated by climate change, resulting in mass-mortality events (Lovelock *et al.*, 2017; Sippo *et al.*, 2018). The role of mangrove mass-mortality events and tree-mediated CH₄ fluxes have not yet been investigated.

Our study aimed to address this gap by quantifying and comparing the CH₄ emissions from both dead and living mangrove tree stems in a region subject to mass mortality of mangroves. We hypothesized that dead mangrove forests (*Avicennia marina*) – lacking root-mediated oxygen transfer and living pneumatophores – may provide a conduit of CH₄ to the atmosphere that enables some bypassing of sediment oxidative processes, and that this pathway is likely a significant component of the net ecosystem CH₄ flux.

Materials and Methods

During late 2015–early 2016, an unprecedented mangrove forest dieback occurred in the Gulf of Carpentaria, Australia, due to climatic extremes (Duke *et al.*, 2017). This resulted in the mortality of 7400 ha of mangrove forest (or *c.* 6% of the Gulf’s mangrove system), extending along *c.* 1000 km of the north Australian coastline (Harris *et al.*, 2017; Sippo *et al.*, 2018). The total dieback area was determined using a combination of remote sensing techniques and field validations, as described in detail by Duke *et al.* (2017). Our sampling took place during 17–26 August 2018, in the winter dry season. We sampled 18 locations either side of the Norman River (17°27′54.63″S, 140°48′58.77″E), where a small patch of living mangroves *Avicennia marina* (Forsk.) Vierh. remained in an area adjacent to large stands of standing dead mangroves (Fig. 1). On average, the tropical, arid region receives rainfall of *c.* 890 mm yr^{−1} which falls mostly during the summer. In August, when this study took place, the long-term average min–max temperatures are 14.0–27.5°C with average precipitation of 2.0 mm (Bureau of Meteorology, 2018).

Sediment redox potentials, sediment methane (CH₄) fluxes and tree stem CH₄ fluxes were measured in upper, middle and lower tidal zones, and replicated along three longitudinal transects (*c.* 300 m each) within dead mangrove forest (T1–T3) and within living mangrove forest (T4–T6) (Fig. 1). The tree stem circumference at breast height (CBH, measured at 130 cm above the sediment) of each sampled standing tree was measured then converted to diameter at breast height (DBH). Tree stem density (trees m^{−2}) was estimated by counting stems of standing trees within duplicate 64-m² quadrats at each site. No downed trees were measured or recorded as part of this study. Standing tree stem CH₄ fluxes were measured via a closed dynamic chamber

technique at height increments of 10, 40, 80 and 170 cm above the ground. The chamber consisted of a 50 mm wide × 40 mm deep plastic cylinder with a silicon flange that was sealed to the tree stems by a circular clay ring, with incubations of 2–3 min duration undertaken at each height increment (Supporting Information Fig. S1). CH₄ fluxes were measured within a closed loop passing through a drying desiccant (DrieriteTM; Xenia, OH, USA), attached to a portable cavity ring-down spectrometer (CRDS) CH₄ analyser (GasScout G4301; Picarro, Santa Clara, CA, USA) recording CH₄ concentration (ppm) changes at 1-s intervals (i.e. ppm s^{−1}). Sediment fluxes were measured using the same approach employing a larger 23 cm wide × 20 cm high circular PVC chamber inserted *c.* 2 cm into the sediment. Because mangrove pneumatophores can act as CH₄ conduits (Purvaja *et al.*, 2004), we avoided measurements from sediments featuring pneumatophores, to avoid potential overestimation of the sediment fluxes. Vertical sediment profiles for redox potentials were measured *in situ* at each site by directly inserting a probe (HachTM HQ40d; Loveland, CO, USA) into freshly extruded 1-m cores, at 5 cm increments to 50 cm depth, and then 10 cm increments to 90 cm depth. Due to the presence of saltwater crocodiles and marine stingers, sampling was restricted to daylight hours, low tide and the dry season.

Methane fluxes (*F*) were calculated for each chamber incubation using the equation:

$$F = (s(V/RT_{\text{air}}A))t, \quad \text{Eqn 1}$$

(*s*, regression slope for each chamber incubation deployments (ppm s^{−1}); *V*, chamber volume (m³); *R*, universal gas constant (8.205 × 10^{−5} m³ atm^{−1} K^{−1} mol^{−1}); *T*_{air}, air temperature inside the chamber (°K); *A*, surface area of the chamber (m²); *t*, conversion factor from seconds to days, and to μmol). To accurately calculate *V* (i.e. total volume of the closed loop including chamber, clay ring, gas tubing, desiccant canister and internal volume of CRDS), a known concentration and volume of CH₄ was injected into the system in the laboratory and volume was calculated as a function of the increase in measured concentration; similar to that described by Siegenthaler *et al.* (2016).

Upscaling flux calculations

In order to upscale fluxes to individual trees, we assumed a simple nonbranching tree with a cylindrical stem. The stem was sectioned into four cylinders (Fig. S1) and the fluxes measured at the corresponding height were applied to the surface area of that height and integrated according to:

$$F_t = \int_0^2 (c \cdot h \cdot F), \quad \text{Eqn 2}$$

(*F*, flux per tree (μmol tree^{−1} d^{−1}); *c*, circumference of the tree at CBH (m); *h*, cylinder height (m); *F*, measured flux rate for that height (μmol m^{−2} d^{−1})). To calculate CH₄ emissions from the ‘normalized’ planar area occupied by each tree stem, we divided *F*_{*t*} by the planar surface area of each tree, calculated from CBH.

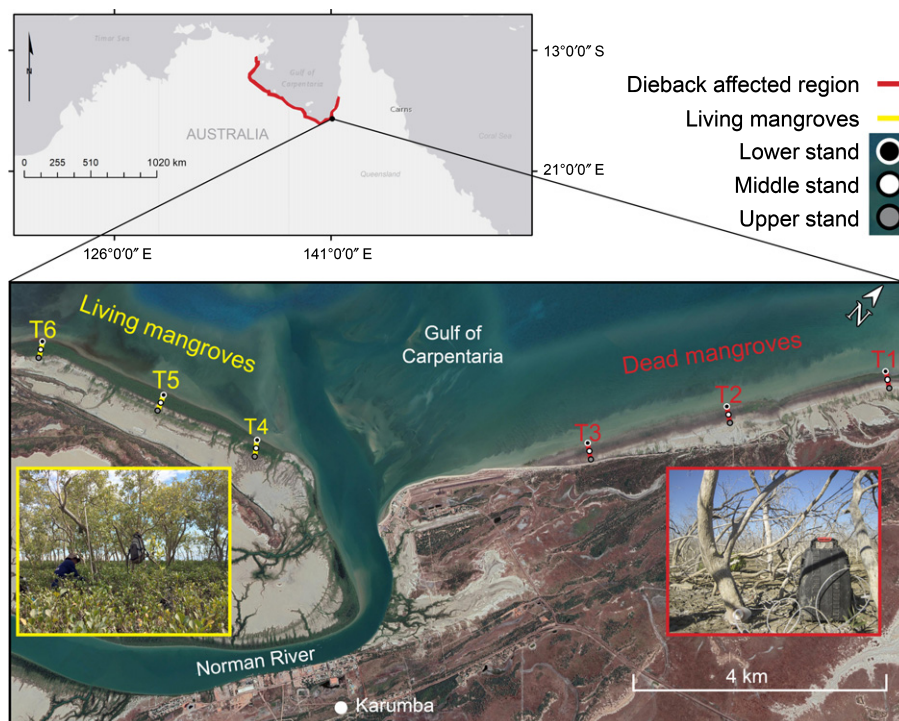


Fig. 1 Study location near Karumba, Queensland, Australia; showing living and dead mangrove forest transects from lower to upper tidal sampling zones. Inset images show healthy living mangrove (T4) and dead mangrove forest (T2).

This assumes a cylindrical stem and therefore may underestimate the tree basal area at the ground surface. To compare our results to other studies, we converted F_t (Eqn 2) to a stem surface area-weighted rate (F_{ta}) which accounts for tree stem surface area ($\mu\text{mol m}^{-2} \text{stem d}^{-1}$) using the equation:

$$F_{ta} = F_t \times (1/T_{sa}), \quad \text{Eqn 3}$$

(T_{sa} , surface area of each tree (m^2), calculated by multiplying CBH (m) by the height of 2 m).

In order to estimate the role of tree stem flux to the net ecosystem CH_4 flux (NEF) (i.e. the sediment flux and tree-stem flux), we first converted to a geometric mean forest area-weighted tree stem flux rate (F_{taw}) for each tidal zone using:

$$F_{taw} = (\text{geometric mean } F_t) \times d \times c, \quad \text{Eqn 4}$$

(d , tree density (trees m^{-2}); c , conversion from $\mu\text{mol d}^{-1}$ to $\text{g ha}^{-1} \text{d}^{-1}$). The sediment fluxes (F_{saw}) were first corrected for the area occupied by tree-stem bases, bioturbation, emergent mangrove seedlings and/or pneumatophores, which each occupied a portion of the sediment flux areal footprints (Table S1). The proportion of nonsediment surface was estimated by counts within $50 \times 50 \text{ cm}$ quadrats ($n = 336$) from upper and lower zones in the dead and living stands (data collected in August 2017). Once corrected, the sediment fluxes were converted to an area-weighted sediment flux ($\text{g-CH}_4 \text{ ha}^{-1} \text{d}^{-1}$) for each tidal zone as per F_{taw} in Eqn 4.

In order to account for the different areal footprints (A_f) of the upper, middle and lower tidal zones (%), we used GIS-derived elevation data of the dead and living stand longitudinal transects.

The total NEF (for dead and living) could then be calculated using the following equation:

$$\text{NEF} = \sum u, m, l (A_f \times F_{taw}) / [\sum u, m, l (A_f \times F_{taw}) + \sum u, m, l (A_f \times F_{saw})], \quad \text{Eqn 5}$$

(u , m and l , upper, middle and lower zones, respectively, for the values of A_f , F_{taw} and F_{saw}). To estimate the total dead tree stem CH_4 emissions due to the mangrove dieback we used the equation:

$$F_{da} = \sum u, m, l [A_f \times F_{taw} \times c], \quad \text{Eqn 6}$$

(F_{da} , flux for the entire dieback area (Mg yr^{-1}); c , conversion to dieback area (7400 ha) and conversion from g d^{-1} to Mg yr^{-1}). We then used the same methods for the living side, assuming that this represented 'baseline emissions', and then subtracted this from the dead side to calculate the change in emissions due to mortality.

Statistics

As the data were nonparametric, Mann–Whitney Rank Sum Tests were performed to test for any significant differences between the living and the dead mangrove stands for tree-stem CBH, sediment redox potentials, sediment CH_4 fluxes and tree-stem CH_4 flux rates. To avoid overestimations in extrapolating our results, calculations relied upon the geometric mean \pm standard error (SE).

Data availability

Data used for the composition of this paper can be obtained from: doi:10.17632/778yzh2cv4.1

Results

The mangrove forest tree stem density was similar between the dieback area (0.17 ± 0.08 trees m^{-2}) and the living forest (0.19 ± 0.07 trees m^{-2}). The average tree DBH also was similar in both areas (10.0 ± 10.7 cm in living stands and 7.8 ± 10.2 cm in the dieback area) but was significantly different (Mann–Whitney Rank Sum Test, $P=0.013$) (Table 1). Average redox potentials in the top 100 cm of sediment revealed decreasing redox potentials with depth (Fig. S2) and from the upper to lower intertidal sediments transects (Fig. 2a), with no significant difference between the dead and living mangrove stands (Mann–Whitney Rank Sum Test, $P=0.25$). The sediment CH_4 fluxes increased with declining redox potential and increased from the upper to lower tidal zone (Fig. 2b; Table 1) and there was no significant difference between the fluxes from dieback sediments and living mangrove sediments (Mann–Whitney Rank Sum Test, $P=0.42$).

The dead tree stem CH_4 flux rates ranged from -90.4 to 4035.7 $\mu mol m^{-2} d^{-1}$ and the living tree stem flux rate ranged from 0.3 to 504.1 $\mu mol m^{-2} d^{-1}$ (Table 1). The mangrove stem CH_4 fluxes were significantly higher from dead vs living mangroves (Fig. S3; Mann–Whitney Rank Sum Test, $P<0.001$), with the average CH_4 flux per dead tree more than eight-fold higher (145.6 ± 25.0 $\mu mol tree^{-1} d^{-1}$) than from living trees (18.2 ± 3.2 $\mu mol tree^{-1} d^{-1}$) (Fig. 2c,d; Table 1). The area-weighted flux rates were 249.2 ± 41.0 and 37.5 ± 5.8 $\mu mol CH_4 m^{-2} stem d^{-1}$ for the dead and living mangrove trees, respectively (Fig. 2e; Table 1). The highest CH_4

fluxes always occurred from the lower 40 cm of each tree stem, then decreased exponentially with height (Figs 2c,d, S4). On average, tree stem CH_4 fluxes increased towards the lower tidal zones; concomitant to both sediment fluxes and redox (Fig. 2e). When the CH_4 fluxes were normalized for the planar area occupied by the tree stems, the average dead mangrove stem fluxes ($23,131 \pm 4173$ $\mu mol m^{-2} d^{-1}$) were more than two orders of magnitude higher than sediment fluxes (185.1 ± 70.9 $\mu mol m^{-2} d^{-1}$), and the planar-normalized living tree fluxes were 4287 ± 642 $\mu mol m^{-2} d^{-1}$, which was 17-fold higher than the living forest sediment fluxes (Table 1).

We estimated that the tidal zones represented 59.8%, 29.7% and 10.5% for upper, middle and lower zones (respectively) of dead zone transects and 50.7%, 34.8% and 14.5% of the living zone transects (Table S2). On the tree-weighted density basis, the area-weighted CH_4 flux from dead forest was 2.82 g- $CH_4 ha^{-1} d^{-1}$, which accounted for 46.3% of the NEF in the upper tidal zone and 6.6% of the NEF in the lower tidal zone (Table 2). For the living stands the area-weighted tree stem flux was 0.35 g- $CH_4 ha^{-1} d^{-1}$ which accounted for 6.7% of the NEF in the upper zone and 2.3% of the NEF in the lower zone (Table 2). When upscaled to the entire dieback region, this resulted in total emission of 7.73 ± 0.83 Mg- $CH_4 yr^{-1}$, which was approximately six-fold more CH_4 than our estimates of living mangrove forest tree stem emissions (0.96 ± 0.57 Mg- $CH_4 yr^{-1}$) for the same area (Table 2).

Discussion

Dead vs living mangrove tree-stem CH_4 emissions

The methane (CH_4) emissions from dead mangrove tree stems were eight times higher than from living trees (Fig. 2c,d,f),

Table 1 Summary of geometric mean and arithmetic mean mangrove tree stem methane (CH_4) flux rates and sediment flux rates from dead and living areas.

Mangrove forest	Average height (cm)	Stem flux range ($\mu mol m^{-2} d^{-1}$)	Geometric mean CH_4 tree stem flux rate ($\mu mol m^{-2} d^{-1}$)	Arithmetic mean CH_4 tree stem flux rate ($\mu mol m^{-2} d^{-1}$)	<i>n</i>	Tidal zone	DBH (cm)	Average density (trees m^{-2})	Geometric mean CH_4 sediment flux ($\mu mol m^{-2} d^{-1}$)	Arithmetic mean CH_4 sediment flux ($\mu mol m^{-2} d^{-1}$)
Dead	12	–90.4 to 4035.7	466.6	1071.1 ± 201.4	38	Upper	9.9	0.18	18.3	31.3 ± 10.4
	40	–63.0 to 1548.7	102.2	246.7 ± 68.4	31	Middle	8.6	0.22	59.8	108.6 ± 32.6
	89	–43.0 to 1053.8	41.6	75.3 ± 30.4	35	Lower	11.3	0.13	222.1	415.6 ± 193.8
	175	4.7 to 322.6	44.9	71.9 ± 14.3	31					
	Mean‡		167.9	249.2 ± 41.0	30	Mean	10.0	0.17	62.5	185.1 ± 70.9
	Flux per tree†		100.4	145.6 ± 25.0	30					
Living	12	0.3 to 504.1	43.8	96.8 ± 27.7	28	Upper	5.6	0.21	23.2	67.3 ± 40.3
	40	0.7 to 164.2	19.9	29.0 ± 7.1	21	Middle	9.2	0.11	105.2	345.2 ± 180.0
	80	7.4 to 114.4	26.2	30.1 ± 4.6	21	Lower	9.9	0.23	270.4	347.7 ± 75.4
	151	12.3 to 62.8	25.6	27.3 ± 2.3	24					
	Mean‡		29.3	37.5 ± 5.8	21	Mean	7.9	0.19	91.6	246.8 ± 67.0
	Flux per tree†		13.2	18.2 ± 3.2	21					

The negative fluxes ($n=10$) occurred in trees featuring holes from borers were included in all calculations (\pm SE), and is the same for geometric and arithmetic means. Symbols: ‡ average rate ($\mu mol CH_4 m^{-2} stem d^{-1}$) calculated using Eqn 3, † represents average CH_4 tree flux ($\mu mol tree^{-1} d^{-1}$) scaled to 2 m height using Eqn 2. DBH, diameter at breast height.

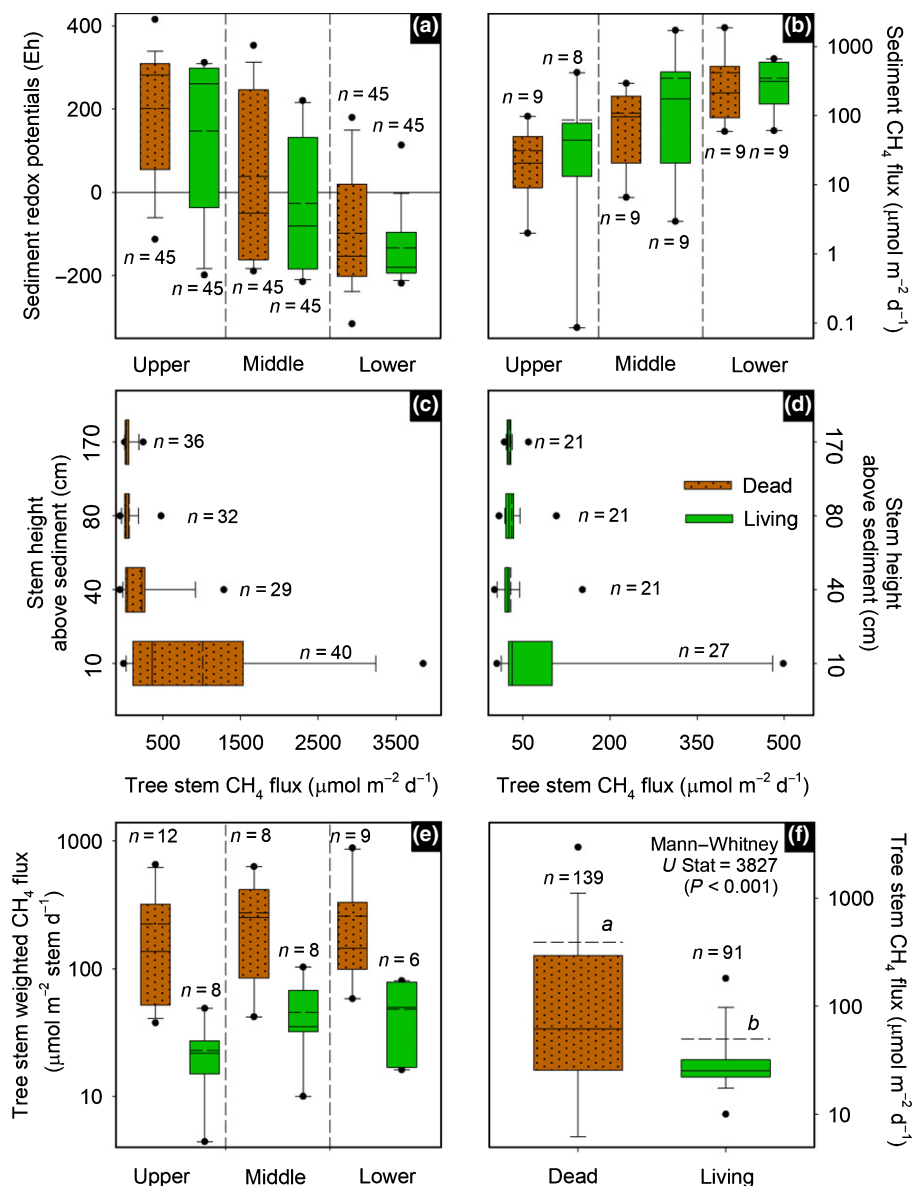


Fig. 2 Box plots showing; (a) sediment redox potentials (Eh) of the top 100 cm sediment for each tidal zone; (b) sediment methane (CH_4) fluxes for each tidal zone; (c) CH_4 fluxes by height of dead mangrove stands; (d) CH_4 fluxes by height of living mangrove stands; (e) individual tree stem weighted CH_4 fluxes for each tidal zones (using Eqn 3), and (f) all CH_4 flux measurements comparison (using Eqn 1). Note: the different x-axes in c and d and the log scale y-axes on b, e and f. *n*, total number of measurements. The mean (dashed line), median (solid line) and dots represent 5th and 95th percentiles.

whereas there was no significant difference in sediment CH_4 fluxes between the dead and living areas (Fig. 2b). This suggests that tree stem flux differences between the dead and living stands were not related to differences between the sedimentary CH_4 pools near the sediment–atmosphere interface. Furthermore, the middle and lower CH_4 sediment fluxes were within range of average global mangrove sediment fluxes of $391.2 \pm 153.4 \mu\text{mol m}^{-2} \text{d}^{-1}$ (Rosentreter *et al.*, 2018). Interestingly, despite mean positive redox potentials of the upper tidal sediments (Fig. 2a), these still sustained relatively important sediment fluxes (Fig. 2b). Although the bulk sediment in this zone was oxidizing, anoxic micro-niches facilitating methanogenesis and/or preferential pathways (i.e. micropores, decaying organic matter and crab burrows) may facilitate CH_4 transport to the surface. We also sampled (where possible) several living trees amongst dead mangroves (T1; Fig. 3) and dead mangroves amongst the living (T5; Fig. 3), yet still found that the highest

CH_4 fluxes came from dead mangrove stems, independent of location (Fig. 3). Furthermore, the average tree stem CH_4 fluxes from both dead and living stands both increased seawards, concomitant with sediment CH_4 fluxes and more reduced sediment profiles, suggestive of sedimentary CH_4 origins (Fig. 2). Therefore, this implies that: (1) the dead tree stems themselves were acting as preferential conduits for CH_4 flux from the sediment to the atmosphere and/or (2) the standing dead trees were a source of CH_4 through methanogenesis occurring within the trees themselves and/or (3) living trees were potentially oxidizing the sedimentary CH_4 pool at the root tip/sediment interface, leading to lower fluxes through living trees.

In mangrove species such as *Avicennia marina*, which are predominant at the Gulf of Carpentaria study site, pressurized stem flow for transporting and storing oxygen is an important adaptation in order to survive tidal inundation and anaerobic sediments (Alongi, 2012; Krauss *et al.*, 2014). This delivers oxygen to the

Table 2 Summary comparing the upscaled dead vs living mangrove methane (CH₄) fluxes and proportion of net ecosystem flux (NEF) by tree-stem CH₄ emissions.

Mangrove forest	Tidal zones	Area (%)	Tree stem CH ₄ flux (g ha ⁻¹ d ⁻¹)*	Sediment CH ₄ flux (g ha ⁻¹ d ⁻¹)*	Tree stem flux contribution to NEF (%)†	Upscaled tree stem CH ₄ flux (Mg yr ⁻¹)‡
Dead	Upper	59.8	2.45	2.87	46.1	4.01
	Middle	29.7	3.71	9.32	28.5	3.01
	Lower	10.5	2.43	34.49	6.58	0.70
	Total		2.82	8.11	25.8	7.73
Living	Upper	50.7	0.23	3.18	6.65	0.31
	Middle	34.8	0.33	14.21	2.29	0.32
	Lower	14.5	0.84	36.07	2.27	0.33
	Total		0.35	11.78	2.90	0.96

Upscaled estimations were calculated using Eqns 4*, 5† and 6‡.

rhizosphere, mitigating the effect of toxic metals and sulfide accumulation near the root tips (Curran, 1985; Hovenden *et al.*, 1995). It is conceivable that active rhizosphere O₂ transport near the root/sediment interface may attenuate CH₄ production and accumulation near the root interface, which may help explain the lower CH₄ fluxes from living tree stems. When tree mortality occurs, water is evacuated from the complex internal hydraulic channels within the trees, spanning from the roots to the atmosphere; leaving an array of empty internal cavities that facilitate upward (nonpressurized) diffusive gas transportation (Carmichael *et al.*, 2018). It is also plausible that a portion of the CH₄ flux from dead stems originates aboveground due to the chemical degradation of plant tissue (Keppler *et al.*, 2006), *in situ* methanogenesis from organic matter decomposition (Covey *et al.*, 2012; Wang *et al.*, 2017), or CH₄ from saprotrophic fungi (Mukhin & Voronin, 2008; Lenhart *et al.*, 2012). However, most studies conclude that the bulk of living tree stem CH₄ emissions originate from the rhizosphere and are either transported upwards through the roots via nonpressurized (diffusion) and/or pressurized processes (xylem and sap flow) (Maier *et al.*, 2018; Barba *et al.*, 2019b). Considering that the dead trees would no longer contain active root systems and the flux rates always decreased upwards along the dead stems (Figs 2, S4), this strongly suggests a belowground CH₄ origin with CH₄ transported via passive diffusion and stem degasification increasing with height (Pitz & Megonigal, 2017; Maier *et al.*, 2018; Barba *et al.*, 2019b).

Internal CH₄ concentrations in dead stems also were assessed by immediately measuring the CH₄ flux from a freshly sawn-off dead mangrove stem at 40 cm height (T3). This revealed a high internal CH₄ concentration of 64 056 ppm providing clear evidence of a positive CH₄ efflux gradient with the atmosphere, a similar result to a study of standing dead freshwater wetland snags (trees) by Carmichael & Smith (2016). Incubations of extracted dead mangrove stem timber found CH₄ flux rates were orders of magnitude lower than the intact stands (Fig. S5). This, therefore, suggests a sedimentary CH₄ origin with stem degasification occurring with height, but also initiates lines for further research whereby isotopic analysis and microbial and fungal ecology may help unravel multiple CH₄ sources.

Comparative CH₄ fluxes

It is challenging to directly compare our CH₄ fluxes to other studies, as most previous work has only measured fluxes at one or two height increments and/or at different heights, seasons, species, freshwater systems and using different methods. To simplify, we compared our average flux rates from ≤ 40 cm of the arid-tropical dead mangrove stems ($714.5 \pm 127.2 \mu\text{mol m}^{-2} \text{d}^{-1}$), to lowland studies measured from similar stem heights (15–50 cm) as summarized in Covey & Megonigal (2019). We found our dead tree stem CH₄ fluxes (from ≤ 40 cm) were *c.* 2–28 times higher than fluxes from living trees from tropical peatland (Pangala *et al.*, 2013), three to four times higher than mature trees of temperate peatland in the UK (Pangala *et al.*, 2015), 0.5–5.8 times that of temperate floodplain trees in Japan (Terazawa *et al.*, 2007, 2015), but were similar to temperate floodplain living trees described in Pitz *et al.* (2018) (Fig. 4). They were, however, much lower than tropical Amazon floodplain tree CH₄ fluxes that were one to two orders of magnitude higher than our data (Pangala *et al.*, 2017). The only other published standing dead tree stem CH₄ emissions ($600 \mu\text{mol m}^{-2} \text{d}^{-1}$), were from a restored coastal freshwater wetland of North Carolina (Carmichael *et al.*, 2018), which was similar to our dead stem fluxes (Fig. 4).

Our average CH₄ fluxes from living mangrove forest stems at ≤ 40 cm height ($69.1 \pm 17.0 \mu\text{mol m}^{-2} \text{d}^{-1}$) were at the low-end of the range of reported tree-stem CH₄ fluxes of previous studies (Fig. 4). This may be partially due to the different sedimentary porewater composition, as saline wetlands (i.e. mangroves) with abundant sulfate composition favour sulfate-reducing bacteria (Burdige, 2012), which partially inhibits sedimentary methanogenesis and thus reduces the subsequent upward tree stem CH₄ emissions. However, temperature, interspecies adaptations and plant physiology likely also play an important role in differences between observed CH₄ flux rates (Pangala *et al.*, 2015). Nevertheless, the data presented here show that CH₄ fluxes through living mangroves tree stems does occur, and should be accounted for in mangrove carbon budgets and blue carbon inventories.

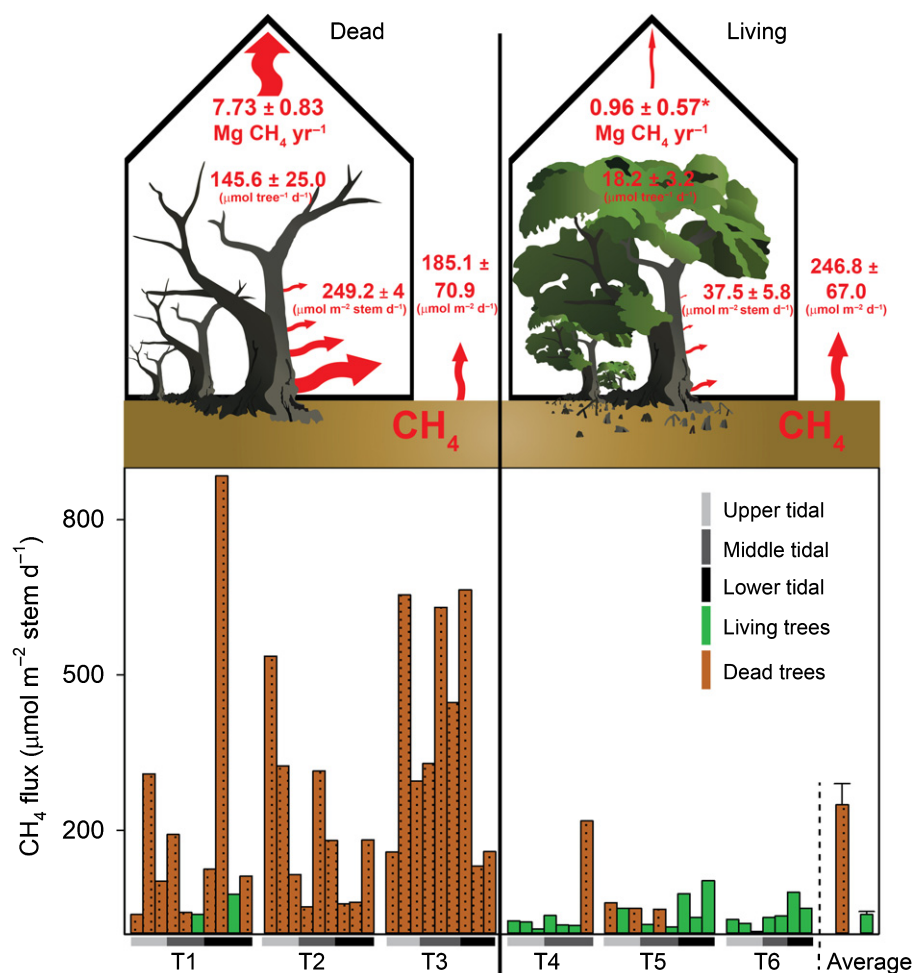


Fig. 3 Conceptual summary of dead vs living mangrove forest showing the upscaled emissions for mortality event area ($\text{Mg CH}_4 \text{ yr}^{-1}$), average tree methane (CH_4) flux to 2 m ($\mu\text{mol tree}^{-1} \text{ d}^{-1}$), average tree stem CH_4 flux rate ($\mu\text{mol m}^{-2} \text{ stem d}^{-1}$) and sediment flux ($\mu\text{mol m}^{-2} \text{ d}^{-1}$). The bottom half shows variability of the individual tree fluxes ($\mu\text{mol m}^{-2} \text{ stem d}^{-1}$ from Eqn 3) for each transect and tidal zone. The error bars represent the standard errors on the average fluxes. Note: * indicates living mangrove tree-stem CH_4 fluxes upscaled to the dieback area for healthy mangrove system comparison.

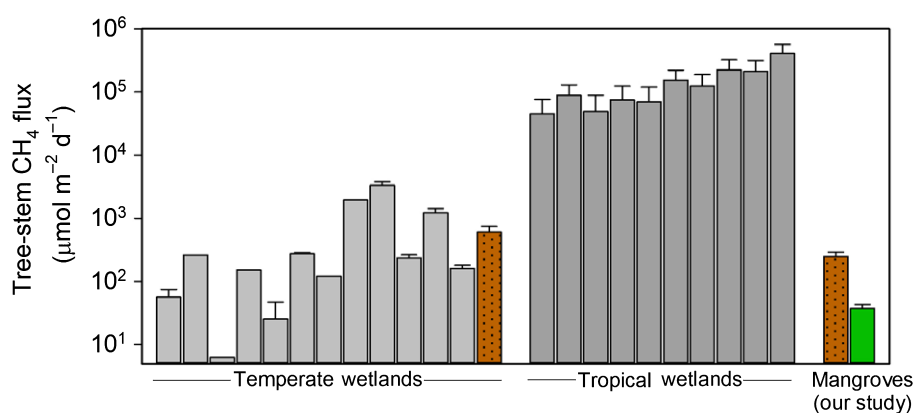


Fig. 4 Comparison of average dead and living mangrove tree stem methane (CH_4) fluxes (our study, Eqn 3) to the range of current literature of wetland tree stem CH_4 fluxes (grey bars) extracted from table 1 in Covey & Magonigal (2019). Note: height measurements and scaling approaches vary amongst studies. Brown symbols with dots represent standing dead trees and \pm SD.

Upscaling the consequence of mangrove forest mortality

We estimated that the dead tree stems emit *c.* 26% of the net ecosystem CH_4 flux (or $2.82 \text{ g CH}_4 \text{ ha}^{-1} \text{ d}^{-1}$) (Table 2). This ratio was within the range of previously reported contributions from a temperate forested freshwater wetland trees (Pangala *et al.*, 2015), but lower than tropical forested

freshwater wetland trees (Pangala *et al.*, 2013). By contrast, the living mangrove tree stem emissions contributed 2.9% of the net ecosystem CH_4 flux. When upscaled to the entire dieback region (7400 ha), dead tree stem CH_4 emissions accounted for $7.73 \pm 0.83 \text{ Mg CH}_4 \text{ yr}^{-1}$, whereas the living mangrove flux scaled to the same surface area would equate to $0.96 \pm 0.57 \text{ Mg CH}_4 \text{ yr}^{-1}$, resulting in a net tree-stem

emissions surplus of $6.77 \text{ Mg CH}_4 \text{ yr}^{-1}$ due to the dieback event (Table 2; Fig. 3).

Although large uncertainties exist within our upscaled results due to our study representing small-scale temporal resolution, our measurements and estimates of both dead and living mangrove stem CH_4 flux should be considered as highly conservative for both this system and (especially) other tropical mangrove systems. This is because (1) the tree density of the tropical-arid Australia Gulf region are about two-thirds lower than systems of similar latitudes (Sanders *et al.*, 2016); (2) we could only account for dry season (tropical) winter sampling (where methanogen microbial metabolism may be lower) which have been shown to have the lowest seasonal sedimentary CH_4 fluxes (Chauhan *et al.*, 2008; Allen *et al.*, 2011); (3) we could not account for diurnal and high tide sampling, which has been shown to emit *c.* 80% higher CH_4 fluxes during high tides from the Sundarban mangroves (Jha *et al.*, 2014); (4) we could not account for branched trees which in some cases may substantially increase the flux per tree estimate; (5) fluxes were only scaled to 2 m in height; and (6) downed tree fluxes were not measured.

Conclusions and future research

Dead mangrove stems clearly emitted significantly more CH_4 than living stems and this novel pathway accounted for *c.* 26% of the dead forest net ecosystem CH_4 flux. Furthermore, living trees also emitted substantial CH_4 to the atmosphere, a finding that has not been reported until now. Although large uncertainties exist with our upscaling approach, the tree-stem CH_4 flux rates presented should be considered conservative over the annual scale due to sampling during the dry season and during low tides where CH_4 fluxes are likely lowest. These data for mangrove forest mortality emissions open up several lines of research, including: investigations of stem CH_4 flux in other mangrove systems; seasonality changes over longer timescales; isotopic analysis to identify potential fractionation and oxidation from $\delta^{13}\text{C}$ - CH_4 source signals; and ascertaining relationships between CH_4 and fungal/ microbial functional group ecology. Future global carbon budgets and in particular blue carbon budgets should account for CH_4 fluxes from living mangrove tree stems, and also consider the potential emissions scenarios and consequences of any future large-scale mangrove mortality events.








Acknowledgements

We thank Alice Gauthy, Geoff Balland and Julia Kalla for fieldwork assistance, and Roz Hagan for laboratory assistance. This work was funded by the ARC (DE1500100581 and DP180101285). DRT acknowledges funding from the ARC which partially funds his salary (DE180100535). We also thank the three anonymous reviewers and the editor Richard Norby for their constructive comments and feedback that helped to strengthen the manuscript. Graphic components used in conceptual model courtesy of the Integration and Application Network, University of Maryland Centre for Environmental Science (www.ian.umces.edu/symbols).

Author contributions

LCJ and DTM conceived the study; DTM and SGJ conceived the methods; LCJ wrote the first draft with reviews and edits from DTM, SGJ, DRT, JZS, YH and GR; and DTM, GR, JZS and YH conducted the fieldwork and data collection.

ORCID

Yota Harada  <https://orcid.org/0000-0002-7734-8801>
Luke C. Jeffrey  <https://orcid.org/0000-0001-6536-6757>
Scott G. Johnston  <https://orcid.org/0000-0002-5826-5613>
Damien T. Maher  <https://orcid.org/0000-0003-1899-005X>
Gloria Reithmaier  <https://orcid.org/0000-0002-9220-3651>
James Z. Sippo  <https://orcid.org/0000-0001-6622-3280>
Douglas R. Tait  <https://orcid.org/0000-0001-7690-7651>

References

- Allen D, Dalal R, Rennenberg H, Schmidt S. 2011. Seasonal variation in nitrous oxide and methane emissions from subtropical estuary and coastal mangrove sediments, Australia. *Plant Biology* 13: 126–133.
- Alongi DM. 2012. Carbon sequestration in mangrove forests. *Carbon Management* 3: 313–322.
- Barba J, Bradford MA, Brewer PE, Bruhn D, Covey K, van Haren J, Megonigal JP, Mikkelsen TN, Pangala SR, Pihlatie M. 2019a. Methane emissions from tree stems: a new frontier in the global carbon cycle. *New Phytologist* 222: 18–28.
- Barba J, Poyatos R, Vargas R. 2019b. Automated measurements of greenhouse gases fluxes from tree stems and soils: magnitudes, patterns and drivers. *Scientific Reports* 9: 4005.
- Bartlett KB, Harriss RC. 1993. Review and assessment of methane emissions from wetlands. *Chemosphere* 26: 261–320.
- Bastviken D, Cole JJ, Pace ML, Van de Bogert MC. 2008. Fates of methane from different lake habitats: connecting whole-lake budgets and CH_4 emissions. *Journal of Geophysical Research: Biogeosciences* 113, G02024. doi: 10.1029/2007JG000608.
- Burdige D. 2012. Estuarine and coastal sediments–coupled biogeochemical cycling. *Treatise on Estuarine and Coastal Science* 5: 279–316.
- Bureau of Meteorology. 2018. *Weather observations of Normanton*. [WWW document] URL <http://www.bom.gov.au/products/IDQ60801/IDQ60801.94266.shtml> [accessed 15 October 2018].
- Carmichael MJ, Bernhardt ES, Bräuer SL, Smith WK. 2014. The role of vegetation in methane flux to the atmosphere: should vegetation be included as a distinct category in the global methane budget? *Biogeochemistry* 119: 1–24.
- Carmichael MJ, Helton AM, White JC, Smith WK. 2018. Standing dead trees are a conduit for the atmospheric flux of CH_4 and CO_2 from wetlands. *Wetlands* 38: 133–143.
- Carmichael MJ, Smith WK. 2016. Standing dead trees: a conduit for the atmospheric flux of greenhouse gases from wetlands? *Wetlands* 36: 1183–1188.
- Chanton JP, Martens CS, Kelley CA. 1989. Gas transport from methane-saturated, tidal freshwater and wetland sediments. *Limnology and Oceanography* 34: 807–819.
- Chauhan R, Ramanathan A, Adhya T. 2008. Assessment of methane and nitrous oxide flux from mangroves along Eastern coast of India. *Geofluids* 8: 321–332.
- Covey KR, Megonigal JP. 2019. Methane production and emissions in trees and forests. *New Phytologist* 222: 35–51.
- Covey KR, Wood SA, Warren RJ, Lee X, Bradford MA. 2012. Elevated methane concentrations in trees of an upland forest. *Geophysical Research Letters* 39. doi: 10.1029/2012gl052361
- Crowther TW, Glick HB, Covey KR, Bettigole C, Maynard DS, Thomas SM, Smith JR, Hintler G, Duguid MC, Amatulli G *et al.* 2015. Mapping tree density at a global scale. *Nature* 525: 201.

- Curran M. 1985. Gas movements in the roots of *Avicennia marina* (Forsk.) Vierh. *Functional Plant Biology* 12: 97–108.
- Donato DC, Kauffman JB, Murdiyarso D, Kurnianto S, Stidham M, Kanninen M. 2011. Mangroves among the most carbon-rich forests in the tropics. *Nature Geoscience* 4: 293.
- Duke NC, Kovacs JM, Griffiths AD, Preece L, Hill DJ, Van Oosterzee P, Mackenzie J, Morning HS, Burrows D. 2017. Large-scale dieback of mangroves in Australia's Gulf of Carpentaria: a severe ecosystem response, coincidental with an unusually extreme weather event. *Marine and Freshwater Research* 68: 1816–1829.
- Harris T, Hope P, Oliver E, Smalley R, Arblaster J, Holbrook N, Duke N, Pearce K, Bindoff N. 2017. Climate drivers of the 2015 Gulf of Carpentaria mangrove dieback. *Earth Systems and Climate Change Hub Report No. 2*. Aspendale, VIC, Australia: NESP Earth Systems and Climate Change Hub.
- Hovenden M, Curran M, Cole M, Goulter P, Skelton N, Allaway W. 1995. Ventilation and respiration in roots of one-year-old seedlings of grey mangrove *Avicennia marina* (Forsk.) Vierh. *Hydrobiologia* 295: 23–29.
- Jha CS, Rodda SR, Thumaty KC, Raha AK, Dadhwal VK. 2014. Eddy covariance based methane flux in Sundarbans mangroves, India. *Journal of Earth System Science* 123: 1089–1096.
- Keppeler F, Hamilton JT, Brass M, Rockmann T. 2006. Methane emissions from terrestrial plants under aerobic conditions. *Nature* 439: 187–191.
- Kirschke S, Bousquet P, Ciais P, Saunio M, Canadell JG, Dlugokencky EJ, Bergamaschi P, Bergmann D, Blake DR, Bruhwiler L *et al.* 2013. Three decades of global methane sources and sinks. *Nature Geoscience* 6: 813–823.
- Krauss KW, McKee KL, Lovelock CE, Cahoon DR, Saintilan N, Reef R, Chen L. 2014. How mangrove forests adjust to rising sea level. *New Phytologist* 202: 19–34.
- Lenhart K, Bunge M, Ratering S, Neu TR, Schüttmann I, Greule M, Kammann C, Schnell S, Muller C, Zorn H *et al.* 2012. Evidence for methane production by saprotrophic fungi. *Nature Communications* 3: 1046.
- Lovelock CE, Duarte CM. 2019. Dimensions of Blue Carbon and emerging perspectives. *Biology Letters* 15: 20180781.
- Lovelock CE, Feller IC, Reef R, Hickey S, Ball MC. 2017. Mangrove dieback during fluctuating sea levels. *Scientific Reports* 7: 1680.
- Maier M, Machacova K, Lang F, Svobodova K, Urban O. 2018. Combining soil and tree-stem flux measurements and soil gas profiles to understand CH_4 pathways in *Fagus sylvatica* forests. *Journal of Plant Nutrition and Soil Science* 181: 31–35.
- McLeod AR, Fry SC, Loake GJ, Messenger DJ, Reay DS, Smith KA, Yun BW. 2008. Ultraviolet radiation drives methane emissions from terrestrial plant pectins. *New Phytologist* 180: 124–132.
- McNicol G, Sturtevant CS, Knox SH, Dronova I, Baldocchi DD, Silver WL. 2017. Effects of seasonality, transport pathway, and spatial structure on greenhouse gas fluxes in a restored wetland. *Global Change Biology* 23: 2768–2782.
- Mukhin VA, Voronin PY. 2008. A new source of methane in boreal forests. *Applied Biochemistry and Microbiology* 44: 297–299.
- Pangala SR, Enrich-Prast A, Basso LS, Peixoto RB, Bastviken D, Hornibrook ER, Sakuragui CM. 2017. Large emissions from floodplain trees close the Amazon methane budget. *Nature* 552: 230.
- Pangala SR, Hornibrook ER, Gowing DJ, Gauci V. 2015. The contribution of trees to ecosystem methane emissions in a temperate forested wetland. *Global Change Biology* 21: 2642–2654.
- Pangala SR, Moore S, Hornibrook ER, Gauci V. 2013. Trees are major conduits for methane egress from tropical forested wetlands. *New Phytologist* 197: 524–531.
- Pitz S, Megonigal JP. 2017. Temperate forest methane sink diminished by tree emissions. *New Phytologist* 214: 1432–1439.
- Pitz SL, Megonigal JP, Chang CH, Szlavecz K. 2018. Methane fluxes from tree stems and soils along a habitat gradient. *Biogeochemistry* 137: 307–320.
- Purvaja R, Ramesh R, Frenzel P. 2004. Plant-mediated methane emission from an Indian mangrove. *Global Change Biology* 10: 1825–1834.
- Rosentreter JA, Maher DT, Erler DV, Murray RH, Eyre BD. 2018. Methane emissions partially offset “blue carbon” burial in mangroves. *Science Advances* 4: eaao4985.
- Sanders CJ, Maher DT, Tait DR, Williams D, Holloway C, Sippo JZ, Santos IR. 2016. Are global mangrove carbon stocks driven by rainfall? *Journal of Geophysical Research: Biogeosciences* 121: 2600–2609.
- Saunio M, Bousquet P, Poulter B, Peregon A, Ciais P, Canadell JG, Dlugokencky EJ, Etiope G, Bastviken D, *et al.* 2016. The global methane budget 2000–2012. *Earth System Science Data* 8: 697–751.
- Siegenthaler A, Welch B, Pangala SR, Peacock M, Gauci V. 2016. Technical Note: Semi-rigid chambers for methane gas flux measurements on tree stems. *Biogeochemistry* 13: 1197–1207.
- Sippo JZ, Lovelock CE, Santos IR, Sanders CJ, Maher DT. 2018. Mangrove mortality in a changing climate: an overview. *Estuarine, Coastal and Shelf Science* 215: 241–249.
- Stocker TF, Qin D, Plattner GK, Tignor M, Allen SK, Boschung J, Nauels A, Bex V, Midgley PM. 2013. *Climate change 2013: the physical science basis. Contribution of Working Group I to the Fifth Assessment Report of the Intergovernmental Panel on Climate Change*. Cambridge, UK: Cambridge University Press.
- Terazawa K, Ishizuka S, Sakata T, Yamada K, Takahashi M. 2007. Methane emissions from stems of *Fraxinus mandshurica* var. *japonica* trees in a floodplain forest. *Soil Biology and Biochemistry* 39: 2689–2692.
- Terazawa K, Yamada K, Ohno Y, Sakata T, Ishizuka S. 2015. Spatial and temporal variability in methane emissions from tree stems of *Fraxinus mandshurica* in a cool-temperate floodplain forest. *Biogeochemistry* 123: 349–362.
- Wang ZP, Han SJ, Li HL, Deng FD, Zheng YH, Liu HF, Han XG. 2017. Methane production explained largely by water content in the heartwood of living trees in upland forests. *Journal of Geophysical Research: Biogeosciences* 122: 2479–2489.
- Warner DL, Villarreal S, McWilliams K, Inamdar S, Vargas R. 2017. Carbon dioxide and methane fluxes from tree stems, coarse woody debris, and soils in an upland temperate forest. *Ecosystems* 20: 1205–1216.

Supporting Information

Additional Supporting Information may be found online in the Supporting Information section at the end of the article.

Fig. S1 Schematic diagram highlighting how CH_4 flux per tree calculations and measurements were made.

Fig. S2 Redox potentials (Eh) for all sites (T1–T6).

Fig. S3 Compiled CH_4 flux data from T1 to T6 showing living (black) vs dead (grey) mangrove CH_4 fluxes at various heights (cm).

Fig. S4 Longitudinal transect data of CH_4 fluxes (T1–T6).

Fig. S5 Image of methods used to test whether CH_4 was being produced *in situ* in the heartwood timber.

Table S1 Parameters used to estimate the proportion of nonsediment surface-to-bare sediment surface area in extrapolating our CH_4 sediment flux results.

Table S2 GIS derived tidal zone areas used in scaling tidal zones for extrapolating our results to the entire dieback region.

Please note: Wiley Blackwell are not responsible for the content or functionality of any Supporting Information supplied by the authors. Any queries (other than missing material) should be directed to the *New Phytologist* Central Office.